

# Transmission Timing and Synchronization Control for Energy-Efficient Multi-Hop LoRaWAN

HIROTO SHIDA, AOTO KABURAKI<sup>1</sup>, (Graduate Student Member, IEEE),  
AND KOICHI ADACHI<sup>1</sup>, (Senior Member, IEEE)

Advanced Wireless and Communication Research Center (AWCC), The University of Electro-Communications, Chofu, Tokyo 182-8585, Japan

Corresponding author: Koichi Adachi (adachi@awcc.uec.ac.jp)

**ABSTRACT** LoRaWAN (Long Range Wide Area Network), a type of LPWAN (Low Power Wide Area Network), has gained popularity for enabling long-distance data transmission with low-power consumption. However, single-hop LoRaWAN may not be able to provide a sufficiently wide communication range in a practical environment. Although multi-hop communication can offer a wider communication range in LoRaWAN, it has its distinct challenges: the hidden node problem, synchronization misalignment, throughput degradation, and increased power consumption due to noncentralized operation. This paper aims to solve those challenges by proposing an autonomous distributed adaptive resource allocation method and a synchronization misalignment compensation method for multi-hop LoRaWAN systems. In the proposed method, each device selects the radio resource, i.e., time slot and frequency channel, for packet transmission through a mapping rule shared among the devices in advance. Since each device can calculate the timing of the current packet transmission from its preceding device, it can compensate for the misalignment of synchronization. Furthermore, predicting the timing of the next packet from the preceding device enables the device to open the receive window during that time only. Thus, this resource selection not only helps avoid packet collisions but also reduces power consumption by preventing unnecessary reception window openings, thereby improving the efficiency of LoRaWAN communication. The proposed methods are implemented in commercially available private LoRa systems to show their potential to reduce device power consumption by up to 50% reduction.

**INDEX TERMS** Internet of Things, LoRaWAN, low-power wide area networks, resource allocation.

## I. INTRODUCTION

### A. BACKGROUND

In recent years, research and development of the Internet-of-things (IoT), in which various devices are connected to the Internet for information exchange, has been underway [2]. Some IoT devices constituting a wireless sensor network (WSN) must be battery-powered for flexible deployment over a wide area to realize smart cities and smart agriculture. Therefore, there is an increasing demand for communication standards that enable long-range communication with low power consumption.

Low-power wide area network (LPWAN) is a generic communication technology that meets the requirements

The associate editor coordinating the review of this manuscript and approving it for publication was Hang Shen<sup>1</sup>.

mentioned above [3]. Although its transmission data rate is low, LPWAN can provide a wide communication area with low power consumption. Since a family of LPWAN technologies uses unlicensed bands, the duty cycle (DC) constraint is introduced on each frequency channel to realize frequency sharing with other systems [4]. The DC is specified for each device and limits the transmission time spent on each frequency channel per unit time below the specified value [5].

Long-range wide area network (LoRaWAN), one of LPWAN technologies, is widely used due to its low deployment cost and use of unlicensed bands. Chirp spread spectrum (CSS)-based long-range (LoRa) modulation is used in the physical layer of LoRaWAN to achieve long-range and low power consumption. In LoRa modulation, the number of bits transmitted per symbol is defined as the spreading factor (SF) in the range of 7 to 12 [6]. Increasing the SF improves noise

immunity and enables long-range communication; the data rate decreases. In other words, a high data rate and long-range communication cannot be achieved simultaneously in a single-hop communication in LoRaWAN.

Multi-hop communication can maintain a high data rate while achieving a wide communication area [7], where several relays are introduced between the transmitter and the receiver. However, we may face several problems if multi-hop communication is introduced to LoRaWAN. First, multi-hop communication is prone to the hidden node problem, in which packet collisions occur due to simultaneous transmissions from devices outside the carrier sense (CS) range [8]. Specifically, suppose the case of LoRaWAN multi-hop communication from a transmitter to relay 1, relay 2, and a receiver in the order. Since the transmitter and relay 2 cannot detect each other's transmission, packet collision may happen. Please note that if they can detect each other, then it is not necessary to introduce relay 1 between them in the first place. Secondly, LoRaWAN devices cannot transmit and receive packets simultaneously due to a half-duplex communication constraint. Lastly, since the relay does not know when a packet will arrive, it always needs to open the receive window to receive the packet that is to be forwarded. This continuous receive window opening drains the battery significantly.

## B. RELATED WORKS

Various approaches have been researched to increase the throughput of multi-hop communications, including time division multiple access (TDMA)-based and spatial division multiple access (SDMA)-based approaches that avoid the hidden/exposed node problem by controlling the transmission timing and beamforming [9], [10], [11]. However, synchronization or beamforming among devices requires communication overhead. Although packet collision can be avoided through request-to-send (RTS) and clear-to-send (CTS) and by using multiple frequencies [12], [13], the number of available frequency channels is limited. Intermittent periodic transmit (IPT) [14] can avoid packet collision along the multi-hop communication path; however, it considers the scenario when all the devices are synchronized, which is not possible in LoRaWAN systems.

Devices should operate with low power consumption to lengthen their battery life. Especially in multi-hop communications, when battery-powered devices such as LoRaWAN devices are used as relays, it is necessary to reduce power consumption. There are two types of approaches to save power consumption in multi-hop communication, namely, time-asynchronous and time-synchronous [15]. In the time-asynchronous approach, each device transmits randomly, and the receiver does not know when a packet will arrive. This can be solved by always opening the receiving window, but the receiver consumes more power than necessary. In [16], the transmitter transmits after receiving a beacon from the receiver, thereby reducing power consumption

by opening a minimum necessary receiving window for the receiver. On the other hand, in the time-synchronous approach, the transmission timing of each transmitter/relay is predetermined, e.g., TDMA-based [17], so the waiting time for packet reception can be significantly reduced. Therefore, it is possible to increase sleep time, which saves power. Since the clocks of low-cost devices in LoRaWAN are not accurate, synchronization deviates among devices over time, i.e., *clock drift* [18]. Thus, it is essential to consider the impact of clock drift in incorporating multi-hop communication into LoRaWAN systems.

## C. PURPOSE AND CONTRIBUTIONS

This paper proposes an autonomous distributed adaptive resource allocation method and a synchronization misalignment compensation method to solve the above problems of conventional multi-hop LoRaWAN. The proposed method dynamically allocates time and frequency resources for packet transmission to avoid packet collision. Specifically, each transmitting device selects one of the available radio resources, i.e., a combination of time slot and frequency channel, based on its hop index and the packet counter in the header of the LoRaWAN packet [6]. This allows the devices to share the resource information for packet collision avoidance. Furthermore, each receiving device can estimate when to receive the next packet, so it does not need to always open the receive window. The estimated transmission timing of its preceding device allows the device to compensate for the impact of clock drift.

The primary contributions of this paper are as follows.

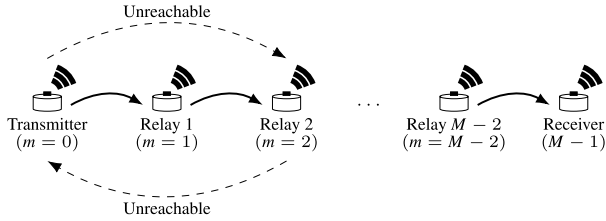
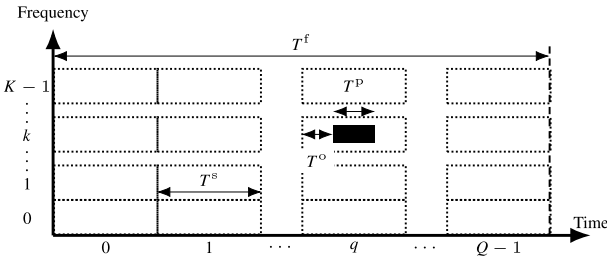
- 1) The proposed resource allocation method can realize efficient LoRaWAN multi-hop communication through dynamic resource mapping based on the device index and the counter index, which enables
  - distributed packet collision avoidance among the devices,
  - and power saving of relays.
- 2) This paper also proposes a sequential synchronization misalignment compensation method among the devices that does not require any control signal overhead.
- 3) The proposed resource allocation method is evaluated through computer simulation and implementation into the commercially available private LoRa devices.

The remainder of this paper is organized as follows. Section II describes the system model. Section III explains the proposed method. Section IV provides the simulation results. Section V shows the actual experimental results. Section VI concludes this paper.

## II. SYSTEM MODEL

### A. TRANSMISSION AND RECEPTION PROCESSES

This paper assumes a multi-hop communication system consisting of  $M$  devices (set  $\mathcal{M} = \{0, \dots, m, \dots, M - 1\}$ ) where data packets are transmitted from a transmitter ( $m = 0$ ) to a receiver ( $m = M - 1$ ) through  $M - 2$  relays ( $m \in$


**FIGURE 1. System model.**

**FIGURE 2. Transmission frame structure.**

$\{1, 2, \dots, M-2\}$ ), as shown in Figure 1. Each device is assigned an index  $m \in \mathcal{M}$  that determines the order of hops, and these indices are assumed to be known among the devices. It is assumed that due to the long distance or obstacles between them, device  $m$  cannot receive the signal from device  $m' (< m-1)$ , which is a practically reasonable assumption.

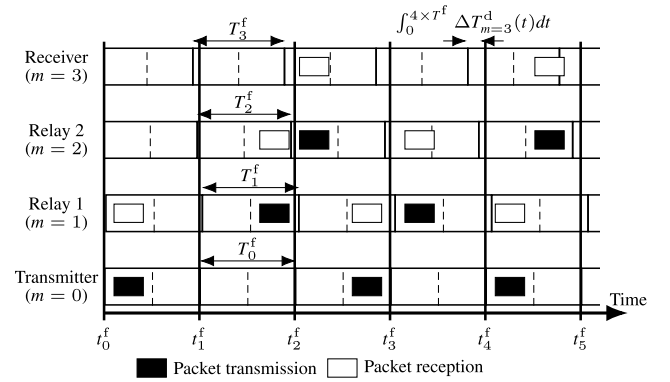
The transmitter sequentially transmits data packets of a fixed time length  $T^p$  sec. Without loss of generality, packet  $i$  contains a packet counter  $i$  in its header.

At the start of transmission, all the relays and receiver (“receiving device  $m_r \in \mathcal{M} \setminus \{0\}$ ”) will be in the standby state with the receive windows of all frequency channels (“all receive windows”) opened until reception of the first packet from the transmitter and their preceding relay (“transmitting device  $m_t \in \mathcal{M} \setminus \{M-1\}$ ”). The relays are able to transmit a packet after receiving the packet from its preceding transmitting device with a smaller index than its own.

As shown in Figure 2, the system divides the continuous time into multiple frames of time length  $T^f$  sec, which is further split into  $Q$  time slots of  $T^s$  sec. The start timing of the  $g$ th frame is denoted by  $t_g^f$ . The system uses  $K$  frequency channels. Thus, the number of available resources within a frame is  $Q \times K$ .<sup>1</sup> Each transmitter selects one of the combinations of time slot and frequency channel, i.e., resource, for packet transmission.

LoRaWAN devices generally operate in a half-duplex mode, meaning transmission and reception cannot be performed simultaneously. Therefore, for example, the transmission timing of a transmitter ( $m=0$ ) and a relay ( $m=1$ ) must be different. In this paper, the devices with even indexes are assumed to transmit in the even-numbered frames, and the devices with odd indexes are assumed to transmit in

<sup>1</sup>Note that since there is no absolute synchronization among the devices, the system is not a kind of Slotted ALOHA system but still a LoRaWAN-compatible system, i.e., ALOHA-like system.


**FIGURE 3. An example of multi-hop communication with clock drift.**

the odd-numbered frames, respectively. In its transmission frame, each device transmits a packet by selecting one time slot within the frame. The packets are transmitted with an offset time  $T^o$  sec from the starting timing in the slot. During the non-transmitting frame, each device can receive a packet from its preceding transmitting device.

## B. CLOCK DRIFT

Since the clocks of inexpensive LPWAN devices are generally not highly accurate, time deviations occur between devices if there is no external input, such as global positioning system (GPS) [19]. Such time discrepancy accumulates over time. This paper defines the clock drift as the relative time deviation of device  $m \in \mathcal{M} \setminus \{0\}$  from device  $m=0$ .

Since the clock drift accumulates over time, the time duration of one frame at device  $m$ , i.e.,  $T_m^f$  sec, can be expressed as [20]

$$T_m^f = T^f + \int_0^{T^f} \Delta T_m^d(t) dt, \quad (1)$$

where  $\Delta T_m^d$  represents the normalized clock drift of device  $m$  normalized by unit time. Similarly,  $T^s$ ,  $T^o$ , and  $T^p$  are set to  $T_m^s$ ,  $T_m^o$ , and  $T_m^p$ , taking into account the clock drift at device  $m$ .

In this paper, the clock at device  $m=0$  is taken as a reference clock, and the relative time deviation of device  $m \in \mathcal{M} \setminus \{0\}$  is considered.

Figure 3 shows an example of multi-hop communication, including the impact of clock drift. As described above (II-A), devices with an even index  $m$  transmit in the even-numbered frames, and devices with an odd index transmit in odd-numbered frames, respectively. In Figure 3, packet collisions will occur if Transmitter and Relay 2 do not select different resources, especially in the even-numbered frame.

Also, due to clock drift, frame time length  $T_m^f$  of device  $m$  becomes either shorter or longer than time length  $T^f$ . Therefore, if synchronization is not performed, transmission and reception across slots will occur in some frames, as shown in Fig. 3, causing packet collisions.

### III. PROPOSED SCHEME

#### A. OVERVIEW

This subsection describes the flow of the proposed method. Figure 4 shows a flowchart of the proposed method for a relay. Note that no receiving procedure for a transmitter and no transmitting procedure for a receiver are necessary, but the rest of the process is the same as that of a relay.

**Transmitter** ( $m = 0$ ) sets the start timing of the 0th frame,  $t_0^f$  sec, and transmits subsequent packets according to the packet transmission procedure described in Section III-A1 at even-numbered frames.

Upon receiving a new data packet from its corresponding transmitter, the relay calculates the frame timing to forward the received packet and to receive the subsequent data packet according to the procedure described in Section III-A2. The above procedure enables the relay to set the sleep time based on the estimated transmission and reception timing according to the procedure in Section III-A2c. Packet transmission is performed in the same way as **Transmitter**, along with the procedure in Section III-A1. Figure 5 shows an example of packet forwarding by the proposed method when devices are ideally synchronized and the number of time slots is  $Q = 2$ . In this example, **Transmitter** ( $m = 0$ ) and **Relay 2** ( $m = 2$ ) transmit in the same even-numbered frames but in different time slots by following the procedure in Section III-A1. Thus, **Relay 1** ( $m = 1$ ) can receive data packets from **Transmitter** ( $m = 0$ ) without the interference from **Relay 2** ( $m = 2$ ). After receiving a packet, **Receiver** ( $m = 3$ ) calculates the frame time to receive subsequent packets according to the packet reception procedure described in Section III-A2.

As mentioned in Section II-B, devices are subject to time deviations due to clock drift. Therefore, this paper proposes a synchronization algorithm that each device carries out based on the information in the header of the LoRaWAN packet in a distributed manner. Upon receiving the first data packet, a device performs initial synchronization as described in Section III-A2a. Then, the device performs sequential synchronization upon the reception of the subsequent data packets, as in Section III-A2b. This compensates for time deviations due to clock drift and enables a transmission/reception method that avoids packet collisions.

#### 1) PACKET TRANSMISSION PROCEDURE

Each device determines the time slot and frequency channel for its packet transmission by using so-called *mapping rules*. Specifically, transmitting device  $m_t \in \mathcal{M} \setminus \{M - 1\}$  determines time slot  $q$  and frequency channel  $k$  in which it transmits packet  $i$  as follows:

$$q(m_t, i) = \text{mod}(f_q(m_t, i), Q), \quad (2)$$

$$k(m_t, i) = \text{mod}(f_k(m_t, i), K), \quad (3)$$

where  $\text{mod}(\cdot, \cdot)$  is the modulo operation,  $f_q(m_t, i)$  and  $f_k(m_t, i)$  are arbitrary functions that produce outputs uniquely determined by index  $m_t$  of the transmitting device and packet counter  $i$ . Since the values of  $i$  and  $m_t$  and mapping

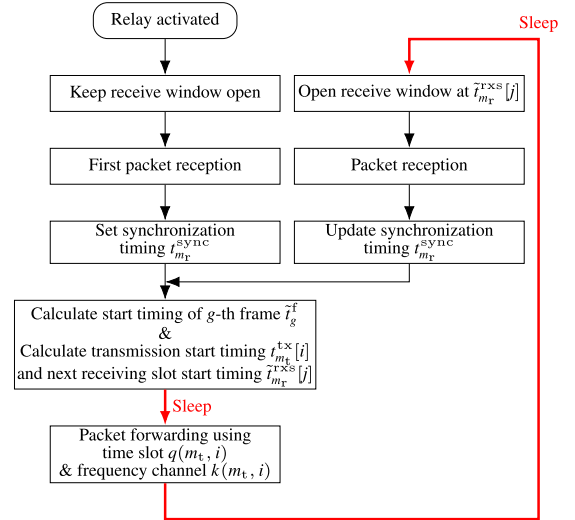


FIGURE 4. Flowchart of the proposed method in relay.

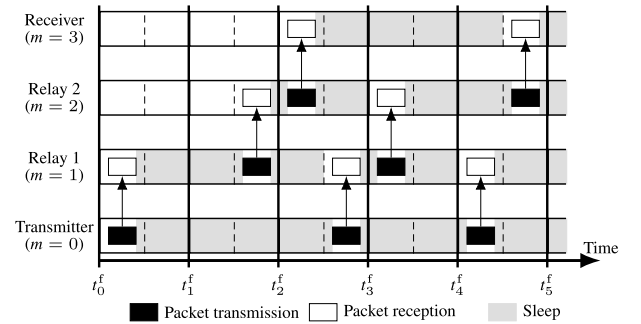


FIGURE 5. Proposed method when each device is synchronized ( $K = 1, Q = 2$ ).

functions (2) and (3) are known by all the devices in the transmission chain, the resource selected by transmitting device  $m_t$  can be obtained by all devices. This paper designs functions  $f_q(m_t, i)$  and  $f_k(m_t, i)$  for targeting collision avoidance, as shown in Figure 6.

The packet transmission start timing,  $t_{m_t}^{tx}[i]$ , is expressed as

$$t_{m_t}^{tx}[i] = \tilde{t}_{m_t}^{txf}[i] + q(m_t, i) \times T_{m_t}^s + T_{m_t}^o, \quad (4)$$

where frame start timing  $\tilde{t}_{m_t}^{txf}[i]$  sec is obtained by (6) in the case of relay. The transmitter calculates  $t_{m_t}^{tx}[i]$  with its own clock from the start timing of the 0th frame  $t_0^f$ .

#### 2) PACKET RECEPTION PROCEDURE

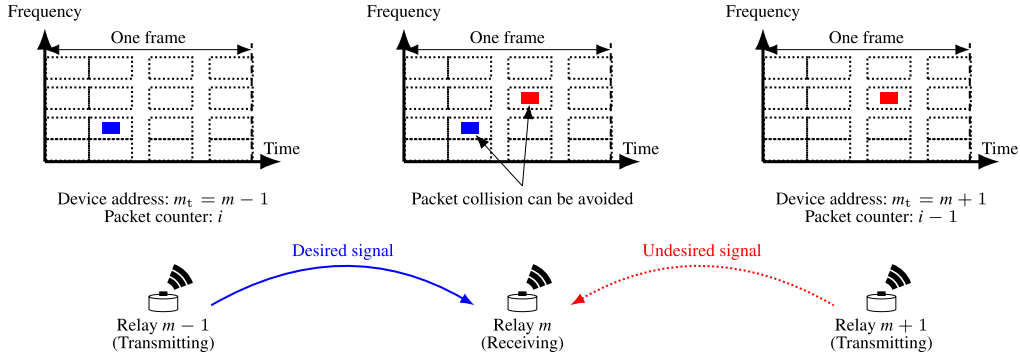
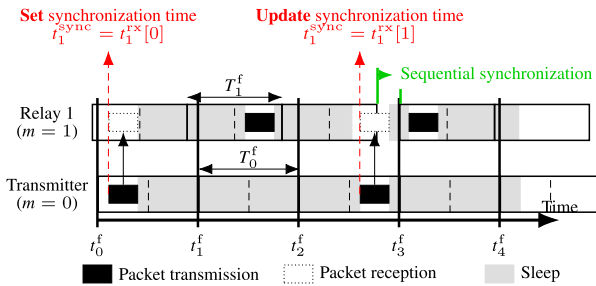
##### a: INITIAL SYNCHRONIZATION

Suppose that receiving device  $m_r \in \mathcal{M} \setminus \{0\}$  receives a packet  $i$  from transmitting device  $m_t = m_r - 1$  at  $t_{m_r}^{rx}[i]$  for the first time, it sets the synchronization timing as  $t_{m_r}^{sync} = t_{m_r}^{rx}[i]$ . Then, the start timing of the  $g$ -th frame  $\tilde{t}_g^f$  is calculated as

$$\tilde{t}_g^f = t_{m_r}^{sync} - T_{m_r}^o - q(m_r - 1, i) \times T_{m_r}^s + (g - 2 \cdot i - m_r + 1) \times T_{m_r}^f. \quad (5)$$

For a relay,  $\tilde{t}_{m_r}^{txf}[i]$  of the frame transmitting received packet  $i$  is calculated as

$$\tilde{t}_{m_r}^{txf}[i] = \tilde{t}_{m_r+2i}^f. \quad (6)$$


**FIGURE 6. Packet collision avoidance through the proposed method.**

**FIGURE 7. Proposed method with sequential synchronization ( $K = 1, Q = 2$ ).**

Receiving device  $m_r \in \mathcal{M} \setminus \{0\}$  calculates the start timing of the receiving slot for next packet  $j$  ( $j > i$ ) as

$$\tilde{t}_{m_r}^{\text{rxs}}[j] = \tilde{t}_{m_r-1+2j}^f + q(m_r - 1, j) \times T_{m_r}^s. \quad (7)$$

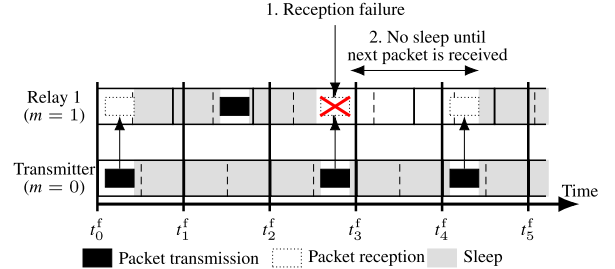
#### b: SEQUENTIAL SYNCHRONIZATION (CLOCK DRIFT COMPENSATION)

Receiving device  $m_r \in \mathcal{M} \setminus \{0\}$  updates the synchronization timing to  $t_{m_r}^{\text{sync}} = t_{m_r}^{\text{rx}}[j]$  once it receives the second or later packet  $j$  ( $j > i$ ) at time  $t_{m_r}^{\text{rx}}[j]$  sec. Then, based on the updated synchronization time  $t_{m_r}^{\text{sync}}$ , it uses (5) ~ (7) to update  $\tilde{t}_g^f$ ,  $\tilde{t}_{m_r}^{\text{rx}}[j]$ , and  $\tilde{t}_{m_r}^{\text{rxs}}[l]$  ( $l > j$ ).

Figure 7 shows an example of the synchronization procedure for Relay 1. Due to the clock drift, frame lengths  $T^f$  of Transmitter and Relay 1 are different. First, Relay 1 performs initial synchronization ( $t_1^{\text{sync}} = t_1^{\text{rx}}[0]$ ) when it receives packet 0 at  $t_1^{\text{rx}}[0]$ . Relay 1 transmits the received packet 0 based on the frame calculated using time  $t^{\text{sync}}[1]$ . Next, when packet 1 is received at time  $t_1^{\text{rx}}[1]$ , it updates the synchronization time  $t_1^{\text{sync}} = t_1^{\text{rx}}[1]$ . Then, the frame timing is recalculated using  $t_1^{\text{sync}}$  to compensate for the clock drift (Sequential synchronization). By updating the frame timing with the sequential synchronization procedure for each packet reception, the synchronization deviation between devices is compensated, and transmission and reception are realized within a given time slot.

#### c: SLEEP TIME CONTROL

Each device reduces its power consumption by switching to sleep during periods when it is not transmitting or receiving. Receiving device  $m_r \in \mathcal{M} \setminus \{0\}$  enters the sleep state and


**FIGURE 8. Sleep time control when packet reception fails ( $K = 1, Q = 2$ ).**

closes all receive windows as soon as the first packet is received from the transmitting device  $m_t \in \mathcal{M} \setminus \{M - 1\}$ . Then, at  $\tilde{t}_m^{\text{rx}}[i]$  (derived from (4)), the device comes out of sleep, forwards the packet, and switches back to sleep. Then, at  $\tilde{t}_m^{\text{rxs}}[i]$  (derived from (7)), the device wakes up from sleep, and waits to receive packets. If a packet is successfully received, it enters the sleep state immediately. On the other hand, if reception does not occur within the estimated receive slot, it waits without sleeping until the next packet is received. Then, upon successful reception, sequential synchronization and sleep time control are performed (Figure 8). Sleep and transmission/reception are repeated in the same manner.

When the second and subsequent packets are received, due to clock drift, the start timing of packet reception  $\tilde{t}_{m_r}^{\text{rx}}[j] = \tilde{t}_{m_r}^{\text{rxs}}[j] + T_{m_r}^o$  predicted by the receiving device and the actual reception timing  $t_{m_r}^{\text{rx}}[j]$  are different. In order to receive packets with consideration of this time discrepancy, the receiving device wakes up from sleep at the start time  $\tilde{t}_m^{\text{rxs}}[i]$  of the receive slot and waits for the reception of packets in the entire receive slot.

## IV. SIMULATION RESULTS

This section provides the computer simulation results to show the performance of the proposed method. Table 1 summarizes the simulation parameters. The frame length,  $T^f$  sec, is determined so that it satisfies duty cycle  $\Delta_{\text{DC}}$  for each frequency channel at each transmitting device as

$$T^f = \frac{T^p}{2K \cdot \Delta_{\text{DC}}}. \quad (8)$$

Since packet length  $T^p$  sec depends on frequency bandwidth  $W$  Hz and spreading factor  $S$ ,  $W = 125$  kHz and

TABLE 1. Simulation parameters.

Parameters	Values
Number of devices, $M$	4
Frame length, $T^f$	2.825 sec
Packet length, $T^p$	{72, 123, 226} msec
Number of frequency channels, $K$	4
Number of time slots, $Q$	2 ~ 40
Duty cycle, $\Delta_{DC}$	0.01
Mean, $[\mu_{min}, \mu_{max}]$	$[-1.91 \times 10^{-3}, 0.28 \times 10^{-3}]$
Variance, $[\sigma_{min}^2, \sigma_{max}^2]$	$[9.59 \times 10^{-11}, 3.19 \times 10^{-10}]$
Consumption current, (transmission) $I^{tx}$	30 mA
Consumption current, (reception) $I^{rx}$	5.5 mA
Consumption current, (sleep) $I^{slp}$	0.9 $\mu$ A
Power supply voltage, $V$	3.3 V

$S = \{7, 8, 9\}$  are used to obtain  $T^p = \{72, 123, 226\}$  msec, which complies with the commercially available private LoRa device [21]. Note that all the devices use the same  $S$ .

The offset time is set to  $T^o = (T^s - T^p)/2$  to transmit a data packet at the center of the time slot. The normalized clock drift  $\Delta T_m^d \sim \mathcal{N}(\mu_m, \sigma_m^2)$  of device  $m$ , with  $\mathcal{N}(\mu_m, \sigma_m^2)$  representing a Gaussian distribution with mean  $\mu_m$  sec and variance  $\sigma_m^2$  sec<sup>2</sup> [20]. Mean  $\mu_m$  and variance  $\sigma_m^2$  used for the clock drift value of each device are determined from uniform random numbers taking the range  $[\mu_{min}, \mu_{max}]$  and  $[\sigma_{min}^2, \sigma_{max}^2]$  of the minimum and maximum values obtained from experimental evaluation, which were obtained through commercially available LoRa devices [20]. Without loss of generality, the arbitrary function used in the proposed method is  $f_q(m_t, i) = f_k(m_t, i) = m_t + i$ . This paper does not consider any packet retransmission.

For evaluating power consumption, consumption current  $I^{tx}$ ,  $I^{rx}$ ,  $I^{slp}$  and power supply voltage  $V$  are set based on the parameters of 920 MHz band radio module [21].

Suppose multiple packets are transmitted simultaneously at the same frequency channel, and a receiving device receives both packets. In that case, we assume that both packets are lost, i.e., no capture effect is taken into account. If a receiving device can receive a packet during the estimated receive window, it is considered that the packet reception is successful.

A. PDR

Here, we will examine the effectiveness of the synchronization compensation of the proposed method. Figure 9 shows the packet delivery rate (PDR) performance as a function of elapsed time. The number of time slots is set to  $Q = 2$ , the minimum number for the proposed method to operate. The PDR is determined by

$$PDR(t) \triangleq \frac{\sum_{u=0}^{U-1} N_u^{suc}(t)}{\sum_{u=0}^{U-1} N_u^{pkt}(t)}, \tag{9}$$

where  $U$  denotes the number of trials,  $N_u^{pkt}(t)$  denotes the total number of packets transmitted by the transmitter up to a certain time  $t$ .  $N_u^{suc}(t)$  denotes the total number of packets

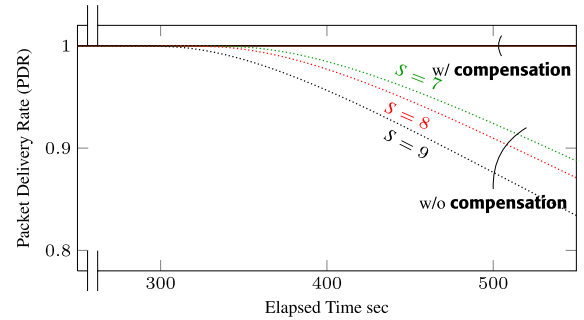


FIGURE 9. PDR performance as a function of elapsed time.

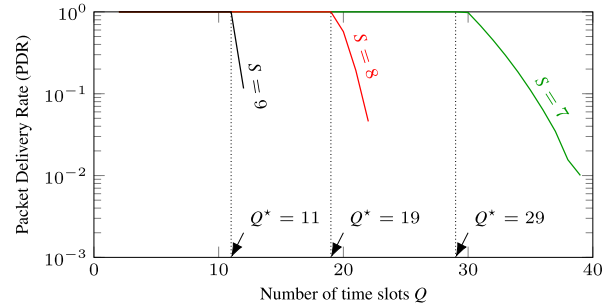


FIGURE 10. The impact of number of time slots  $Q$  on PDR performance.

the receiver can receive until a certain time  $t$ . The PDR performance with the proposed sequential synchronization (clock drift compensation) is denoted as “w/ comp.”, and the case without sequential synchronization is denoted as “w/o comp.”. The proposed sequential synchronization method can keep the PDR to 1 regardless of  $S$ . However, if the clock drift compensation is not introduced, the PDR performance begins to drop after a certain period of time. This is because the accumulated clock drift prevents packets from fitting into the expected receive slots at the receiving device, resulting in a drop in PDR. Furthermore, the PDR drops earlier when  $S$  is large, indicating that the system is more susceptible to clock drift.

Next, the effect of number of time slots  $Q$  on the PDR performance is shown in Figure 10. Increasing number of time slots  $Q$  leads to more sleep time, but it shortens time slot length  $T^s$  and time offset length  $T^o$  within each time slot, which makes the system less robust against the clock drift.

In LoRa, the larger  $S$  becomes, the longer  $T^p$  becomes. In this system with fixed-length time slots, the larger  $S$  becomes, the more susceptible the system becomes to clock drift, and the earlier the PDR performance starts to drop. In particular, for the considered simulation parameters,  $S = 9$  can keep PDR of 1 up to  $Q^* = 11$ ,  $S = 8$  up to  $Q^* = 19$ , and  $S = 7$  up to  $Q^* = 29$ . If  $Q$  is increased beyond these values, the clock drift value cannot be absorbed and the PDR will start to drop.

B. POWER CONSUMPTION

Next, the power-saving effect of the proposed method is evaluated. The power consumption during transmission state  $W^{tx}$ , reception state  $W^{rx}$ , and sleep state  $W^{slp}$  are shown in

**TABLE 2.** The power consumption during transmission, reception, and sleep.

	Transmission $W^{\text{tx}}$	Reception $W^{\text{rx}}$	Sleep $W^{\text{slp}}$
Power consumption	99 mW	18.15 mW	2.97 $\mu$ W

Table 2. The power consumption is calculated as the product of current  $I$  and supply voltage  $V$  for each state.

Since relays do not know the reception timing of the data packet in multi-hop communication, it is necessary to keep the receive window open to receive the data packet. Thus, the scenario when the relays always open the receive window is considered for comparison, i.e., *comparison method*. On the other hand, the proposed method enables the relay to estimate the packet reception time from its corresponding transmitter, so it can reduce power consumption by switching to a sleep state.

First, the power consumption during a transmission state,  $J^{\text{tx}}$ , can be calculated as

$$J^{\text{tx}} = W^{\text{slp}} \times (T^f - T^p) + W^{\text{tx}} \times T^p, \quad (10)$$

where each relay becomes sleep mode except for packet transmission duration  $T^p$  in a transmission frame. This value is the same for both the proposed and comparison methods.

Next, the power consumption during the reception mode of the proposed method,  $J_{\text{prop}}^{\text{rx}}$ , is calculated as

$$J_{\text{prop}}^{\text{rx}} = W^{\text{slp}} \times (T^f - T^s) + W^{\text{rx}} \times T^s. \quad (11)$$

Since the proposed method enables each relay to estimate the time slot to receive a data packet, except for the packet reception, the relay can switch to the sleep state. On the other hand, in the comparison method, relays must always open the receive window during the entire reception frame, so the power consumption during the reception frame,  $J_{\text{comp}}^{\text{rx}}$ , is expressed as

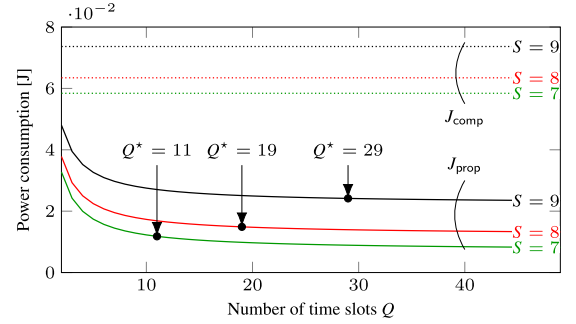
$$J_{\text{comp}}^{\text{rx}} = W^{\text{rx}} \times T^f. \quad (12)$$

Thus, the power consumption required to forward one packet at each relay can be calculated for the proposed method,  $J_{\text{prop}}$ , and the comparison method,  $J_{\text{comp}}$ , respectively as

$$J_{\text{prop}} = J^{\text{tx}} + J_{\text{prop}}^{\text{rx}}, \quad (13a)$$

$$J_{\text{comp}} = J^{\text{tx}} + J_{\text{comp}}^{\text{rx}}. \quad (13b)$$

The power consumption required to forward one packet at each relay is plotted as a function of  $Q$  in Figure 11 with  $S$  as a parameter. If the proposed method is not applied, a constant amount of power is consumed regardless of  $Q$  because the relay always opens the receive window. For smaller  $S$ , packet transmission time  $T^p$  becomes shorter, and hence transmission power consumption  $J^{\text{tx}}$  becomes smaller. As a result, overall power consumption  $J_{\text{comp}}$  is smaller. For the proposed method, receive power consumption  $J_{\text{prop}}^{\text{rx}}$  becomes smaller as  $Q$  increases because of shorter time slot

**FIGURE 11.** Power consumption required for one packet forwarding as a function of  $Q$ .

length  $T^s$ , meaning larger  $Q$  is preferred from the viewpoint of power consumption.

However, as Figure 10 shows, the PDR performance deteriorates for larger  $Q$  due to the clock drift. We can say that there is a tradeoff between the power consumption reduction and PDR performance. Thus, the power consumption  $J_{\text{prop}}$  with  $Q^*$  in Figure 10 is the minimum power consumption the proposed method can achieve. For the simulation parameters considered, the proposed method reduces the energy consumption by about 84.7% (at  $Q^* = 29$ ) for  $S = 7$ , 76.5% (at  $Q^* = 19$ ) for  $S = 8$ , and 63.3% (at  $Q^* = 11$ ) for  $S = 9$ , compared to the system without proposed method.

## V. EXPERIMENTAL MEASUREMENT

This section reports the implementation results of the proposed method on commercially available devices and provides indoor experimental results of multi-hop communication using the proposed method. Each device alternates between transmitting and receiving at each frame. Each device selects one resource from multiple resources in a frame to transmit or receive: the mapping formulas, (2) and (3), are shared among the devices in advance and used for time slot and frequency channel selection.

### A. COLLISION AVOIDANCE MAPPING MEASUREMENT

#### 1) EXPERIMENTAL ENVIRONMENT

Figure 12 shows the experimental environment for the collision avoidance mapping measurement, presented in Section V-A. The 920 MHz band radio module ES920LR2 produced by EASEL and the evaluation board ES920EB were used as devices (Transmitter, Relay 1, Relay 2, and Receiver). Each device was connected to a PC to store the communication logs. This connection was used for storing the log only and each device was working on its own internal clock. A spectrum analyzer connected to a PC was used to monitor the spectrum of each device. Each device is equipped with an antenna, and the transmission power is set to a different value for each device for monitoring purposes (Table 3). Please note that the performance of the proposed method and its effectiveness are not affected by the locations of devices and the distances between them. Thus, for the ease of experimental carryout, we adopted the experimental setup as shown in Figure 12.

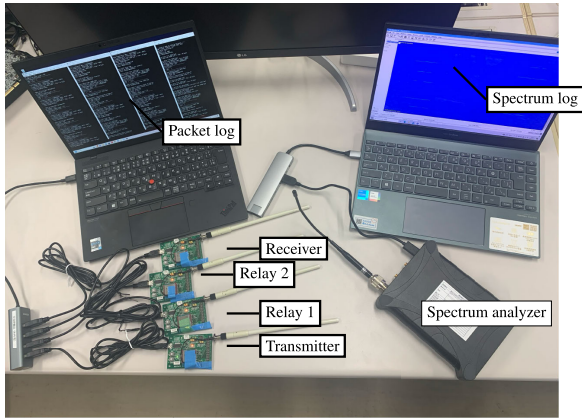


FIGURE 12. Experimental environment for Collision avoidance mapping.

TABLE 3. Transmission power of device.

	Transmitter	Relay 1	Relay 2
Transmission Power	13 dBm	-4 dBm	7 dBm

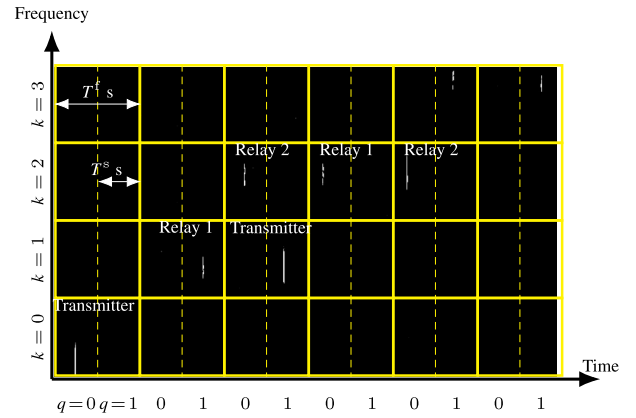
2) EXPERIMENTAL RESULTS

The experimental results are provided in this section. First, Figure 13 shows an example of transmission mapping when the number of time slots is  $Q = 2$  and the number of frequency channels is  $K = 4$ . This is an example of multi-hop communication with sufficient transmission resources. Each device switches transmission and reception every  $T^f$  sec. The mapping formula, (2) and (3) are used to adaptively select time slot  $q$  and frequency channel  $k$  for each packet transmission. This allows Transmitter and Relay 2, which are assumed to be in a hidden node relationship, to transmit data packets in the same frame while avoiding packet collision at Relay 1. Furthermore, Relay 1 can open the receive window so that it can receive the next packet from Transmitter only. In the example shown in Figure 13, sfTransmitter and Relay 2 selected resources that were orthogonal to each other in time and frequency because there were sufficient resources for selection. In practice, packet collision avoidance is possible if either time or frequency is different. The proposed method works as long as the number of resources ( $Q \times K$ ) within a frame is at least two.

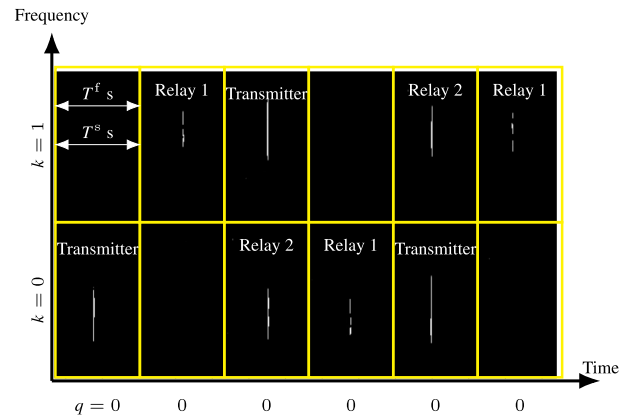
Next, two examples where the number of resources within a frame is two are shown in Figures 13(b) and 13(c). First, Figure 13(b) shows the situation when there is only one time slot but two frequency channels, i.e.,  $T^f = T^s$ . Transmitter and Relay 2 can avoid packet collision by selecting different frequency channels by using (2) and (3), to avoid collisions. Next, Figure 13(c) shows the situation when there is only one frequency channel but there are two time slots. In this scenario, packet collision avoidance is realized by selecting different time slots.

B. CURRENT MEASUREMENT

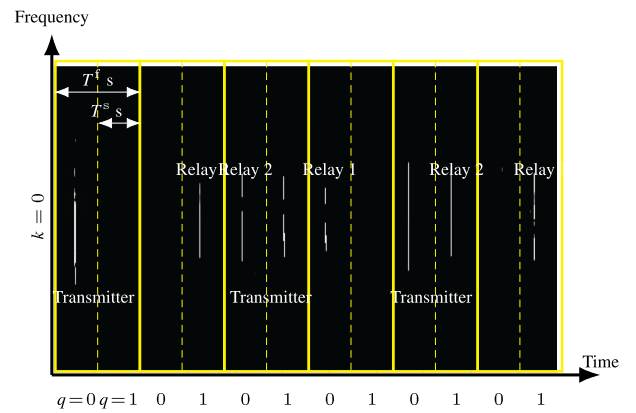
In this implementation, an experimental multi-hop communication system is established using four devices: one transmitter, two relays, and one receiver. Figure 14 shows



(a)  $Q = 2, K = 4$  (Two time slots per frame)



(b)  $Q = 1, K = 2$  (One time slot per frame)



(c)  $Q = 2, K = 1$  (Two time slots per frame)

FIGURE 13. Transmission mapping of each device (Color and aspect ratio corrected). The solid yellow broad line shows the boundary of the time frame and frequency channel while the dotted yellow line shows the boundary of time slot within a time frame.

the experimental environment for Current measurement in Section V-B. The 920 MHz band radio module ES920LR2 from EASEL and the evaluation board ES920EB were used for each device, and communication logs were checked on a PC. Relay 1 is connected to a USB tester to measure current consumption and voltage.

The measurement results of the current consumption of Relay 1 that receives packets from Transmitter and forwards

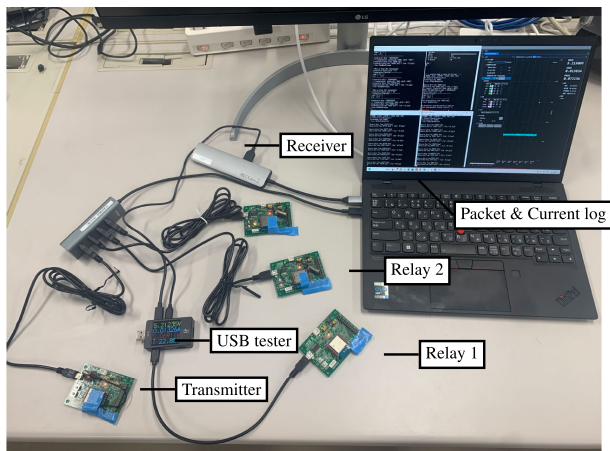


FIGURE 14. Experimental environment for current measurement.

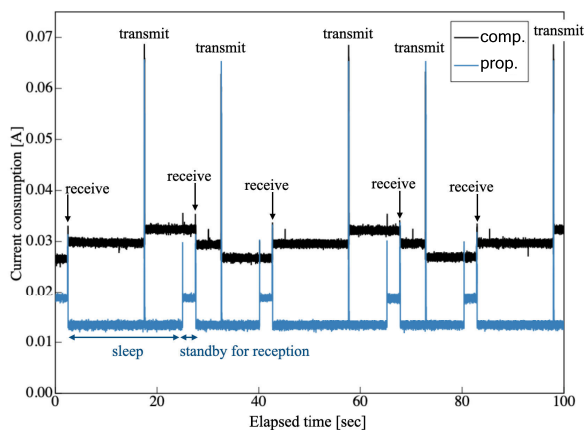


FIGURE 15. Current consumption of elapsed time.

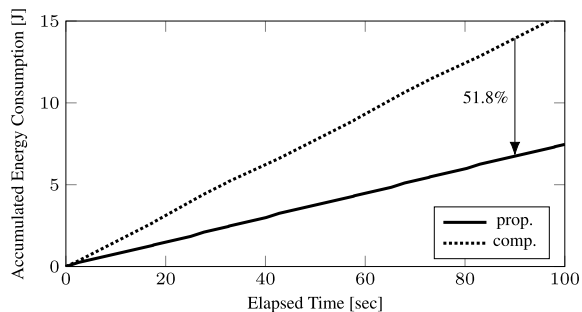


FIGURE 16. Cumulative power consumption as a function of elapsed time.

them to Relay 2 are shown in Figure 15. The frame length is set to  $T^f = 10$  sec, and the number of time slots is set to  $Q = 1$  without loss of generality.

The proposed method is labeled as “prop.” and the comparison method is labeled as “comp.”, in which the receive window is always open except when sending packets. Generally, the current is higher during transmission and reception states than during sleep state and standby state, so the peaks are higher. The comparison method (comp.) requires each relay to always open the receive window because it does not know when the packet will arrive, which results in a higher current. On the other hand, the proposed method (prop.) enables the relays to predict the time slot and

frequency channel in which a packet will arrive. It can be confirmed from Figure 15 that the current consumption rises temporarily at the start of the receive standby and enters the sleep state immediately after the reception is completed. This indicates that the proposed method (prop.) is able to take a longer time for sleep mode.

Next, the accumulated energy consumption of Relay 1 is shown in Figure 16. The power consumption is calculated by integrating the product of the current consumption measured in Figure 16 and the power supply voltage (5.23 V) over time. Both methods show a linear increase in cumulative power consumption with elapsed time. The proposed method (prop.) shows a more gradual increase than the compared method (comp.), reducing cumulative power consumption by about 51.8%. This enables battery-powered relay devices such as LoRaWAN devices to continue operating for nearly twice as long as the comparison method.

## VI. CONCLUSION

This paper proposed an autonomous distributed adaptive resource allocation method and a synchronization misalignment compensation method to solve the hidden node problem, synchronization misalignment, throughput degradation, and increased power consumption in a LoRaWAN multi-hop communication. In particular, the proposed method maps transmission resources using the index of the order of hops and the packet counter that can be obtained from the received packet. Sharing the transmission resources selected by each device among the devices in a distributed manner enables the devices to avoid packet collisions and open the receive window only when it is necessary. Through experiments on actual equipment, the operation of the proposed mapping method that enables synchronous processing and collision avoidance, as well as the reduction of power consumption, was demonstrated. Implementing the proposed method in a commercially available private LoRa system has shown up to 50% reduction of the device power consumption compared to the system without the proposed method.

In this paper, we have considered a single-chain of the multi-hop communication link of LoRaWAN, which is a practical setup scenario to extend the communication distance of the LoRaWAN system. However, we also acknowledge the scenario where multiple transmitters or relays transmit packets to a relay. Extending the proposed approach to such a scenario is an important research direction. Furthermore, this paper did not consider packet retransmission that can enhance the reliability of LoRaWAN communication. Although incorporating packet retransmission into the proposed method can significantly improve communication reliability, a careful resource selection algorithm should be developed as the proposed method relies on the packet counter for resource allocation. An unexpected packet collision may happen if the packet is lost during relaying. Thus, incorporating packet retransmission into the proposed method is an interesting future work.

## ACKNOWLEDGMENT

An earlier version of this paper was presented in part at the 2024 ICNC [DOI: 10.1109/ICNC59896.2024.10555925].

## REFERENCES

- [1] H. Shida, A. Kaburaki, and K. Adachi, "Energy-efficient multi-hop LoRaWAN with transmission and synchronization control," in *Proc. Int. Conf. Comput., Netw. Commun. (ICNC)*, Feb. 2024, pp. 1104–1108.
- [2] A. Ikpehai, B. Adebisi, K. M. Rabie, K. Anoh, R. E. Ande, M. Hammoudeh, H. Gacanin, and U. M. Mbanaso, "Low-power wide area network technologies for Internet-of-Things: A comparative review," *IEEE Internet Things J.*, vol. 6, no. 2, pp. 2225–2240, Apr. 2019.
- [3] P.-M. Mutescu, A. I. Petriariu, and A. Lavric, "Wireless communications for IoT: Energy efficiency survey," in *Proc. 12th Int. Symp. Adv. Topics Electr. Eng. (ATEE)*, Mar. 2021, pp. 1–4.
- [4] K. Mikhaylov, "On the uplink traffic distribution in time for duty-cycle constrained LoRaWAN networks," in *Proc. 13th Int. Congr. Ultra Modern Telecommun. Control Syst. Workshops (ICUMT)*, Oct. 2021, pp. 16–21.
- [5] 920 MHz-Band Telemeter, *Telecontrol Data Transmission Radio Equipment*, Standard ARIB STD-T108, 2021.
- [6] LoRa Alliance Tech. Committee. (2020). *LoRaWAN 1.1 Specification*. [Online]. Available: [https://loro-alliance.org/wp-content/uploads/2020/11/lorawantm\\_specification\\_v1.1.pdf](https://loro-alliance.org/wp-content/uploads/2020/11/lorawantm_specification_v1.1.pdf)
- [7] M. O. Farooq, "Multi-hop communication protocol for LoRa with software-defined networking extension," *Internet Things*, vol. 14, Jun. 2021, Art. no. 100379.
- [8] Z. Cao, H. Jin, and J.-B. Seo, "Hidden node probability in LoRa with listen-before-talk," *IEEE Wireless Commun. Lett.*, vol. 13, no. 10, pp. 2917–2921, Oct. 2024.
- [9] A. Sgora, D. J. Vergados, and D. D. Vergados, "A survey of TDMA scheduling schemes in wireless multihop networks," *ACM Comput. Surveys*, vol. 47, no. 3, pp. 1–39, Apr. 2015.
- [10] J. Dias and A. Grilo, "Multi-hop LoRaWAN uplink extension: Specification and prototype implementation," *J. Ambient Intell. Humanized Comput.*, vol. 11, no. 3, pp. 945–959, Mar. 2020.
- [11] F. Ono and K. Sakaguchi, "MIMO spatial spectrum sharing for high efficiency mesh network," *IEICE Trans. Commun.*, vol. 91, no. 1, pp. 62–69, Jan. 2008.
- [12] T. Luo, M. Motani, and V. Srinivasan, "CAM-MAC: A cooperative asynchronous multi-channel MAC protocol for ad hoc networks," in *Proc. 3rd Int. Conf. Broadband Commun., Netw. Syst.*, Oct. 2006, pp. 1–10.
- [13] H. Zhai, J. Wang, and Y. Fang, "DUCHA: A new dual-channel MAC protocol for multihop ad hoc networks," *IEEE Trans. Wireless Commun.*, vol. 5, no. 10, pp. 3224–3233, Nov. 2006.
- [14] H. Furukawa, "Hop count independent throughput realization by a new wireless multihop relay," in *Proc. IEEE 60th Veh. Technol. Conf.*, vol. 4, Sep. 2004, pp. 2999–3003.
- [15] A. Bachir, M. Dohler, T. Watteyne, and K. K. Leung, "MAC essentials for wireless sensor networks," *IEEE Commun. Surveys Tuts.*, vol. 12, no. 2, pp. 222–248, 2nd Quart., 2010.
- [16] T. Hatauchi, Y. Fukuyama, M. Ishii, and T. Shikura, "A power efficient access method by polling for wireless mesh networks," *IEEJ Trans. Electron., Inf. Syst.*, vol. 128, no. 12, pp. 1761–1766, 2008.
- [17] G. Leenders, G. Callebaut, G. Ottoy, L. Van der Perre, and L. De Strycker, "An energy-efficient LoRa multi-hop protocol through preamble sampling for remote sensing," *Sensors*, vol. 23, no. 11, p. 4994, May 2023.
- [18] J. Haxhibeqiri, I. Moerman, and J. Hoebeke, "Low overhead scheduling of LoRa transmissions for improved scalability," *IEEE Internet Things J.*, vol. 6, no. 2, pp. 3097–3109, Apr. 2019.
- [19] C. Garrido-Hidalgo, J. Haxhibeqiri, B. Moons, J. Hoebeke, T. Olivares, F. J. Ramirez, and A. Fernández-Caballero, "LoRaWAN scheduling: From concept to implementation," *IEEE Internet Things J.*, vol. 8, no. 16, pp. 12919–12933, Aug. 2021.
- [20] K. Tsurumi, A. Kaburaki, K. Adachi, O. Takyu, M. Ohta, and T. Fujii, "Simple clock drift estimation and compensation for packet-level index modulation and its implementation in LoRaWAN," *IEEE Internet Things J.*, vol. 9, no. 16, pp. 15089–15099, Aug. 2022.
- [21] *Specified Low Power Radio Module ES920LR2 Data Sheet Version 1.05*, Standard ES920LR2, 2022.



**HIROTO SHIDA** received the B.E. and M.E. degrees in information and communication engineering from The University of Electro-Communications, Japan, in 2022 and 2024, respectively. His research interest includes low-power wide area networks.



**AOTO KABURAKI** (Graduate Student Member, IEEE) received the B.E. and M.E. degrees in information and communication engineering from The University of Electro-Communications, Japan, in 2020 and 2022, respectively, where he is currently pursuing the Ph.D. degree. His research interest includes machine learning and its application to wireless communication.



**KOICHI ADACHI** (Senior Member, IEEE) received the B.E., M.E., and Ph.D. degrees in engineering from Keio University, Japan, in 2005, 2007, and 2009, respectively.

From 2007 to 2010, he was a Japan Society for the Promotion of Science (JSPS) Research Fellow. He was a Visiting Researcher with the City University of Hong Kong, in April 2009. He was a Visiting Research Fellow with the University of Kent, from June 2009 to August 2009. From May 2010 to May 2016, he was with the Institute for Infocomm Research, A\*STAR, in Singapore. Currently, he is an Associate Professor with The University of Electro-Communications, Japan. His research interests include cooperative communications and energy efficient communication technologies.

Dr. Adachi is a member of IEICE. He was recognized as an Exemplary Reviewer from IEEE WIRELESS COMMUNICATIONS LETTERS, in 2012, 2013, 2014, and 2015. He received the Excellent Editor Award from IEEE ComSoc MMTC, in 2013. He is the co-author of WPMC2020 Best Student Paper Award. He served as the General Co-Chair for the Tenth and 11th IEEE Vehicular Technology Society Asia Pacific Wireless Communications Symposium (APWCS); the Track Co-Chair for Transmission Technologies and Communication Theory of the 78th and 80th IEEE Vehicular Technology Conference, in 2013 and 2014, respectively; the Symposium Co-Chair for Communication Theory Symposium of IEEE Globecom 2018 and Wireless Communications Symposium of IEEE Globecom 2020; and the Tutorial Co-Chair for IEEE ICC 2019. He was an Associate Editor of *IET Transactions on Communications* (2015–2017), *IEEE WIRELESS COMMUNICATIONS LETTERS* (since 2016), *IEEE TRANSACTIONS ON VEHICULAR TECHNOLOGY* (2016–2022), *IEEE TRANSACTIONS ON GREEN COMMUNICATIONS AND NETWORKING* (2016–2021), *IEEE OPEN JOURNAL OF VEHICULAR TECHNOLOGY* (since 2019), *IEEE Transactions on Wireless Communications* (since 2023), and *IEEE Communications Surveys and Tutorials* (since 2023).

• • •